White Paper

June 2017

Characterization of Modal Dependence of MMF Chromatic Dispersion for Wideband MMF

Presented at the 64th IWCS Cable and Connectivity Symposium, Atlanta GA, October 5-8, 2015

PANDUIT®

Overview

The rapid growth of network traffic requires ever higher data rates in the data center. The development of (short reach) cost effective Ethernet and Fibre Channel communication links operating at data rates more than 100 Gb/s over a single fiber will require wavelength division multiplexing (WDM) using multi-wavelength VCSEL transceivers capable of serial data rates ≥25 Gb/s.

Transceivers using four wavelengths in the 850 - 950nm spectral window are under development for a new generation of 100 Gb/s duplex transmission. However, the bandwidth of current OM4 MMF, designed to operate in the 850±10nm window, will not support the required reach with these new transceivers.

To design a new wideband multimode fiber, the effects of the modal and chromatic dispersion need to be considered. The effect of launch condition on the chromatic dispersion (CD) can become more relevant since it is a source of noise that can restrict accurate CD characterization. This is more relevant now since the TIA study group responsible for developing SWDM using a new type of MMF has started a CD R&R Round Robing among main suppliers of MMF solutions [4].

The launch dependence of MMF CD measurement has been previously studied [1-3]. However, the impact of MMF mode groups (MG) on CD has not been studied experimentally. Moreover, the previously applied models do not accurately represent the VCSEL sources, laser optimized MMF, nor the wide bandwidth MMF currently under development for multiple wavelength transmission [4]. Recently, we reported the CD dependence on MMF mode groups [5] where we utilized a measurement system similar to standard differential mode delay (DMD) measurements. The output of a single-mode launch fiber was coupled to a MMF at increasing radial offsets, while the test wavelength was varied from 850nm to 1400nm to measure the mode group zero dispersion wavelength and dispersion slope [5]. The reported results, which provided an accurate method to estimate the relative variation of CD among mode groups. However, the reported method did not provide the accuracy required to estimate the absolute value of the dispersion slope.

In this paper, we improved the accuracy of both the absolute values of CD and its variation among modes. Our measurement set-up consists of a supercontinuum white light source with a narrow temporal width pulse (6 ps FWHM), a monochromator, a computer controlled offset launch mechanism, and a sampling scope with an Agilent* 86105C photodetector plugin module. Using this set-up, it is possible to observe high accuracy and repeatability of the zero dispersion wavelength and dispersion slope of the majority of the mode groups excited in the MMF.

FBAT03--WW-ENG, Rev 0, 06/2017

MMF Chromatic Dispersion Measurement – Current Standard Method

MMF chromatic dispersion measurement and analysis and reporting of results are standardized by international standards bodies [7]. One of the four possible methods is spectral group delay in time domain, which is also the reference method for MMFs. In Figure1 an example of current standard MMF CD measurement is shown. With the standard measurement, an overfilled launch excites all the MMF modes, and the group delay as a function of wavelength is calculated simply as the centroid of temporal pulse. It is noted that the group delay gets noisy as the modal dispersion increases at longer wavelengths. The standard model for group delay curve fit is a three-term equation, but a five-term equation can also be used.

A closer investigation of individual mode group delays as a function of wavelength reveals that mode groups show different chromatic dispersion (both different zero dispersion wavelength and slope). In the following sections, we investigate modal dependence of CD theoretically and experimentally.

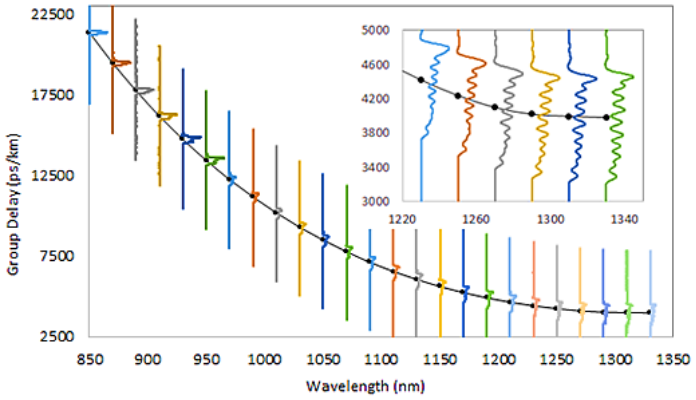

Figure 1. Standards based MMF chromatic dispersion measurement: Group delays calculated at each wavelength as the pulse centroid, which is then curve fitted to Sellmeier coefficients for λo and So. Centroid gets noisy around λo.

Modeling and Experimental Study of Modal Dependence of Chromatic Dispersion on MMFs

Modeling and experiment results presented in this paper show that each mode group of the MMF has a distinct zero dispersion wavelength. Previous models of launch dependence on MMF CD have utilized local CD associated with radial dependence of the index profile such as described in [1]. There are several limitations with that model for current or next generation laser optimized fibers since it uses an approximation that depends on the refractive index profile, but not on the dopant properties. Moreover, it cannot predict the λ_0's of the mode groups of the fiber. A different approach based on theory is developed for alpha-profile MMF as summarized below.

Modeling of Zero Dispersion Wavelengths in Alpha-Profile Refractive Index MMF

MMFs with alpha-profile refractive index are commonly used to model high performance multimode channels. The refractive index profile of these MMFs inside the core is described by a function given by [5],

$$n = n_1\sqrt{1-2\Delta\left(\frac{r}{a}\right)^{\alpha}} \tag{1}$$

where, $\Delta \sim (n_1\text{-}n_2)/n_1$, is the refractive index contrast, n_1 is the refractive index on the axis of the fiber, n_2 is the refractive index in the cladding, r is the radial position inside the fiber core, a is the core raduis, and α is the exponent parameter which takes a value of ~ 2 for fibers designed to support operation near 850nm. A simplified expression for the mode group delay, t_g, as a function of the wavelength is obtained below [5],

$$t_g(\lambda,\alpha) = \frac{N_1(\lambda)}{c} + t_R(g,\lambda,\alpha) \tag{2}$$

where N_1 is the group refractive index and where g is the mode group (MG) index, and, $t_R(g,\lambda,\alpha)$ is the relative mode group delay given by,

$$t_R(g,\lambda,\alpha) = \frac{N_1(\lambda)}{c}\Delta\left(\frac{\alpha-\alpha_{opt}(\lambda)}{\alpha+2}\right)\cdot\left(\frac{v_g}{v_T}\right)^{\alpha/(\alpha+2)} \tag{3}$$

where v_g is the number of modes inside the MG, v_T is the total number of modes, $k_0 = 2\pi/\lambda$ and λ is the optical source wavelength, and,

$$\alpha_{opt}(\lambda) = 2 - \frac{2n_1}{N_1}\frac{\lambda}{\Delta}\frac{d\Delta}{d\lambda} \tag{4}$$

For a MMF with Ge dopant in the core at a given concentration, (3) and a determined spectral range $\alpha_{opt}(\lambda)$ can be approximately estimated using,

$$\alpha_{opt}(\lambda) \approx 2 - A\lambda^2 - \frac{B}{\lambda^2} - C \tag{5}$$

where A, B, and C represent parameters that depend on the dopants concentration. Using (5) in (3) and if the number of modes inside in each mode group is proportional to the square of the MG index, we obtain,

$$t_R(g,\lambda,\alpha) = \frac{N_1(\lambda)}{c}\Delta\left(\frac{\alpha-2+A\lambda^2+B/\lambda^2+C}{\alpha+2}\right)\cdot\frac{g}{MG_{\max}} \tag{6}$$

where MG_{max} is the maximum number of MG allowed to propagate in the MMF.

The derivative of $t_R(g,\lambda,\alpha)$ with respect to the wavelength can be approximated to,

$$\frac{dt_R(g,\lambda,\alpha)}{d\lambda} \approx \frac{N_1(\lambda)}{c}\Delta\left(2A\lambda - 2B/\lambda^3\right)\cdot\frac{g}{MG_{\max}} \tag{7}$$

Previous equation indicates that for known amount of Ge concentration the mode group delays scale proportional with the wavelength and the MG. The zero dispersion wavelengths for each MG can be obtained making the derivative of (2) equal to zero, as given below,

$$\frac{d\{t_g(\lambda,\alpha)\}}{d\lambda} = \frac{d\{N_1(\lambda)\}}{cd\lambda} + \frac{d\{t_R(g,\lambda,\alpha)\}}{d\lambda} = 0 \tag{8}$$

Using (7) in (8)

$$\frac{d\{t_g(\lambda,\alpha)\}}{d\lambda} \approx D_M + \frac{N_1(\lambda)}{c}\Delta\left(\frac{2A\lambda - 2B/\lambda^3}{\alpha+2}\right)\cdot\frac{g}{MG_{\max}} = 0 \tag{9}$$

where D_M is the material dispersion at the fiber core.

Since α_{opt}, Δ, and N_1 can be obtained from the Sellmeier coefficients [8] of the dopants used in the fiber, equation (9) provide a general method to estimate the zero dispersion wavelength of each mode group as a function of the alpha parameter and characteristic of the dopants.

In general, we can express (9) as,

$$\frac{d\{t_g(\lambda,\alpha)\}}{d\lambda} \approx D_M + S_A \cdot g\lambda - \frac{S_B \cdot g}{\lambda^3} = 0 \tag{10}$$

where

$$S_A = \frac{N_1(\lambda)}{c}\Delta\left(\frac{2A}{\alpha+2}\right)\cdot\frac{1}{MG_{\max}} \tag{11}$$

$$S_B = -\frac{N_1(\lambda)}{c}\Delta\left(\frac{-2B}{\alpha+2}\right)\cdot\frac{1}{MG_{\max}} \tag{12}$$

We use the three term Sellmeier model approximation [7] to estimate the chromatic dispersion,

$$D_M = \frac{S_o}{4}\lambda\left(1-\left(\frac{\lambda_z}{\lambda}\right)^4\right) \tag{13}$$

where S_0 is the dispersion slope, and λ_z is the zero dispersion wavelength.

Using (11) in (10)

$$\frac{S_o}{4}\lambda\left(1-\left(\frac{\lambda_z}{\lambda}\right)^4\right) + S_A g\lambda - \frac{S_B g}{\lambda^3} = 0 \tag{14}$$

Grouping the equation terms properly, it is possible to find

$$\left(\frac{S_o + 4S_A g}{4}\right)\lambda\left(1-\left(\frac{(\lambda_z^4 + S_B g)/(1+\frac{4S_A g}{S_o})}{\lambda^4}\right)\right) = 0 \tag{15}$$

For Ge doped MMF, we neglect S_B since $\lambda_z^4 >> S_B$. From (15) we can estimate the dispersion slope and zero dispersion wavelength for each mode group as shown below,

$$S_o^{'}(g) = S_o + 4S_A g \tag{16}$$

$$\lambda_z^{'}(g) = \lambda_z / (1 + \frac{4Sg}{S_A})^{0.25} \tag{17}$$

This simple, analytical model represented in equations 16-17 can be used to estimate the effect that the mode groups have in the dispersion slope $S_o^{'}(g)$ and zero dispersion wavelength $\lambda_z^{'}(g)$.

The simplified model indicates that the dispersion slope increases as the mode group increases while the zero dispersion wavelength decreases as the MG increases. The magnitude of these variations will depend on the dopant composition of the MMF.

For example, for a fiber with relatively high concentration of GeO_2 in the core (11.7 mol%) and without cladding dopants S_A=7.86211E-05 producing increase of S_0 as high as 6.04%. At the same time, the zero dispersion wavelength will reduce in about 1.5%.

As an example, for a MMF with less dopant concentration at the core we use GeO_2 5 4.5 mol%.
To maintain an index contrast of about 1% we use 2% wt of F on the cladding. This produces S_A=2.75597E-05, and an increase of about 2.11% from the MG g=0 to g=17. For the same fiber and MGs, the zero dispersion wavelength is expected to change in about 0.5%.

For evaluation of S_0 and λ_z as a function of radial offsets, a more complex computational model is required to simulate the DMD pulses from a controlled offset launch using a single mode fiber (SMF) [6]. Here we used the WKB method to model the complete chromatic and modal delays for fiber doped only with Ge in the core and F in the cladding.

In Figure 2, modeled group delays, $\tau g(\lambda)$ at each radial offset [0-25 micron] are plotted as function of wavelength (radial offset group delays are calculated from mode group delays using p-matrix). Calculated group delays are curve fitted according to [7] to calculate the corresponding λ_o and S_o, which are plotted in Figure 3.

Figure 3 illustrates the complete range of values for S_o and λ_o that can be achieved at any launch condition. This means that the (S_o, λ_o) coordinates for the overfill, underfill and EF launch will result in values somewhere along the radial offset data points.

For example, for the MMF #4 with SMF launch at the center of the MMF core, the model estimates that (S_o, λ_o) will take values of (0.094 ps/nm/km^2, 1325nm). An overfill launch for this fiber can produce up to 20nm shorter λ_o and higher S_o.

The dashed and dotted traces in this plot represent the lines of constant value for the dispersion parameters D. Note that S_o-λ_o curves as radial offset varies, do not follow the constant D lines. Dispersion varies with launch radial offsets (therefore mode groups). For the MMF 4 shown in the graph the change in D from zero radial offset to 25 micron offset is about 2.3 ps/km/nm.

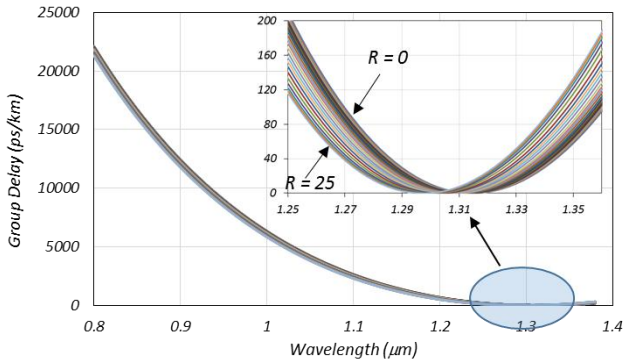

Figure 2. Modeled radial offset group delays (calculated from mode group delays using p-matrix), 8.7% GeO_2 in the core and F in the cladding (MMF 2 in Figure 3.)

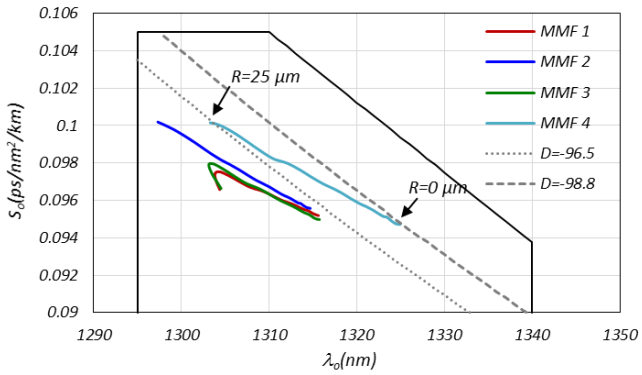

Figure 3. Modeled λ_o and S_o, for different mode groups and radial offsets for 4 MMFs with GeO_2 core dopant concentration between 11.5 to 8.7 mol%. The fiber with highest $Ge0_2$ concentration is the MMF #4.

Zero Dispersion Wavelength and Dispersion Slope Measurements

Our measurement set-up consists of a supercontinuum white light source with a narrow temporal width pulse (6 ps FWHM), a monochromator, a computer controlled offset launch mechanism, and a high-speed sampling scope with an Agilent 86105C photodetector plugin module. Six MMFs representing a variety of OM3, OM4 of 1km length each from three different manufacturers are tested.

Figure 4 depicts the radial offset chromatic dispersion measurement method employed in our set-up. Narrow temporal pulse from the supercontinuum source is passed through the monochromator to output around 5-6nm spectral width (FWHM) for the wavelength range of 830-1360nm. The resultant optical signal is coupled to a standard single mode fiber that scans across the MMF at 1 micron steps. The output of the MMF is then coupled to the sampling scope optical plug-in module, triggered by the white light source. The resultant waveforms as shown in Figure 4 are identical to DMD waveforms, except in this case the wavelength is scanned across a suitable CD measurement wavelength range.

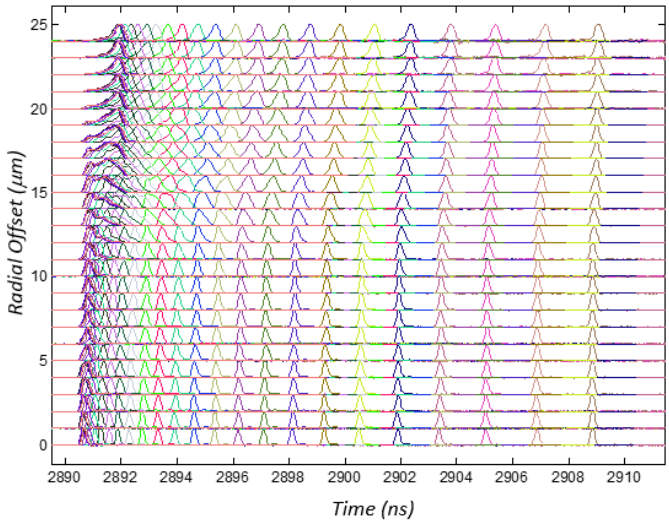

Figure 4. Example of MMF radial offset CD measurement. Resultant waveforms are similar to standard DMD waveforms (wavelength range: 850-1400nm).

As an example, in Figure 5a we show the DMD profiles of the fiber at a wavelength of 1270nm. The DMD profiles are measured following standardized test procedures for DMD measurements. A temporally short and spectrally narrow pulse (reference pulse) from a SMF is launched into the core of the MMF at several radial offsets and resultant pulses are measured after propagating through the MMF under test [6]. However, it should be noted that our procedure differs from the Standards in that the DMD profile is measured for all wavelength between 830nm to 1360nm in 10nm steps.

As an illustrative example one radial offset, 10μm, is selected in which at least five MGs can be observed. The group delays as a function of the wavelength for all the MG present in this radial offset is shown in Figure 5b. A line connecting the centroid of each MG is shown to represent the group delay variation as a function of wavelength for nine wavelengths. It can be observed that for each MG the delays reduce or increased as the wavelength changes. However, at the zero dispersion wavelength of each MG (circle marks) the derivative of t_g is zero.

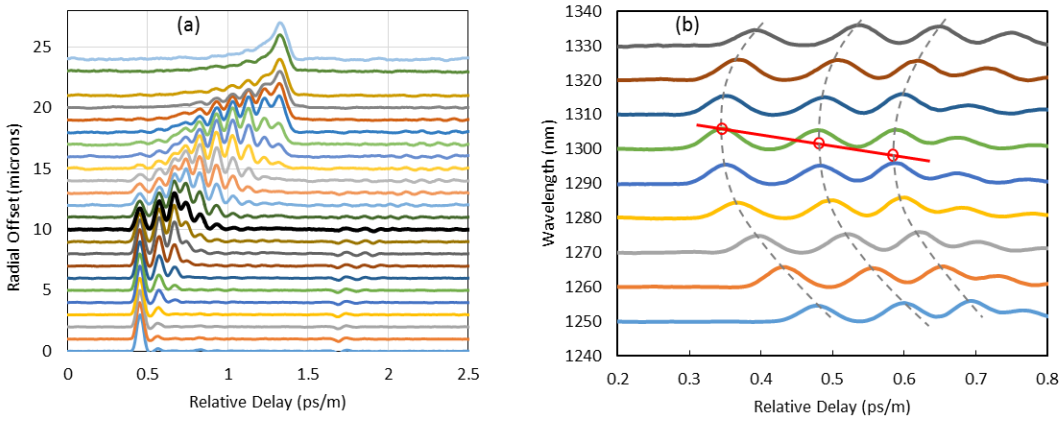

Figure 5. (a) DMD profile measured at 1270nm for a fiber with modal bandwidth of 4500 MHz.km at 850nm (b) Example showing different chromatic dispersion for different exited MG group delay (red circles are the λo's).

Finally, the measurements on six different MMFs are shown in Figure 6. The set of fibers studied here cover samples from three major MMF manufacturers, and standard, bend optimized and wideband versions, with varying modal bandwidth performance. When S_o is plotted vs λ_o, (a generally accepted way to look at chromatic dispersion), a clear trend is observed. The lower radial offsets (LOMs) show longer λ_o and lower S_o compared to higher radial offsets (HOMs) regardless of MMF type and manufacturer. Another important feature in Figure 6 is that the S_o-λ_o curves of MMFs do not line up with constant dispersion curves (an example is shown as dotted line for -97.5 ps/nm/km dispersion). The LOMs and HOMs show about 4 ps/nm/km dispersion difference (see Figure 9 for more details). All six fibers show similar S_o/λ_o slopes.

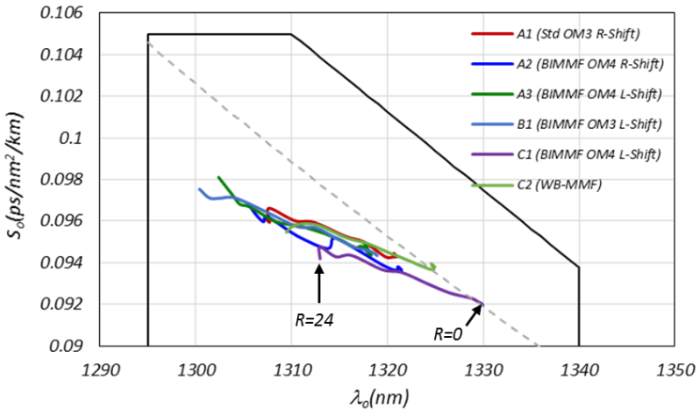

Figure 6. S_o is plotted vs. λ_o at different offsets (0-24 microns, 2 micron radial offset steps) for six different MMFs, from three manufacturers. LOMs corresponding to lower radial offsets show increased λ_o and reduced slope, while HOMs behave conversely.

CD from Arbitrary Launch Condition: Scaling the Offset Launch Data

To study the launch condition effect, we utilize radial modes instead of MG. This approach avoids the challenges of tracking the variations of each MG in the broad spectral region measured, and more importantly relates directly with methods already developed for the modal bandwidth characterization of MMF [6].

The procedure to compute λ_o and S_o from the waveform resultant of each radial offset excitation is described as follows. The center wavelength of the pulses resultant of the radial offset excitation are computed. The values of λ_o and S_o are computed from the center wavelength as defined in the Standards procedure [7].

The CD parameters measured at each radial offset ($\lambda_o(r)$, $S_o(r)$) are used to calculate overall λ_o and S_o, by weighting the radial offset values with total power at that offset.

$$\lambda_o = \frac{\int_0^a P(r)\lambda_o(r)dr}{\int_0^a P(r)dr} \qquad S_o = \frac{\int_0^a P(r)S_o(r)dr}{\int_0^a P(r)dr} \tag{18}$$

Similarly, the total dispersion of the MMF can be calculated using,

$$D = \frac{\int_0^a P(r)D(r)dr}{\int_0^a P(r)dr} \tag{19}$$

where $P(r)$ represents the power excited at each radial offset by the input source, and therefore represents the launch condition utilized. For example, when the power is launched only at the center of the fiber, denoted here as SM launch, $P(r) = 1$ only when $r = 0$. This procedure is applied to measured radial offset data for the six fibers with overfilled and ten VCSEL weights. Figure 7 shows a comparison of standard overfilled launch based CD with the OFLc weighted calculations (OFLc weights are well known in industry and are used to estimate MMF overfilled bandwidth from standard DMD measurements [6]). Recognizing that the two are from two different actual measurements and there is an expected variation due to repeatability and reproducibility of CD measurements, the two results are very similar for both λo and So.

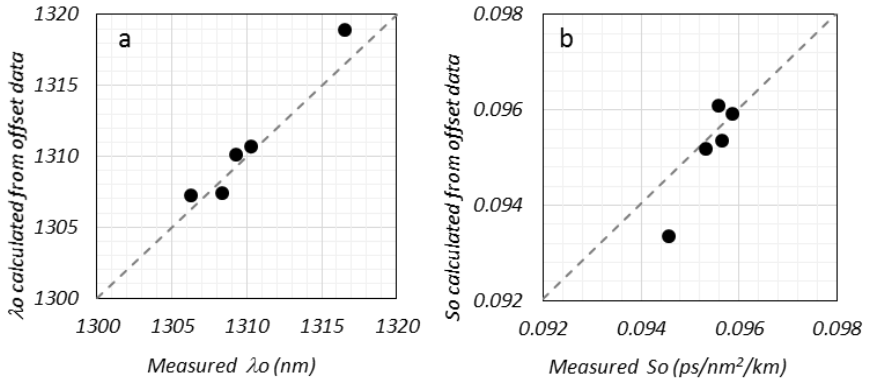

Figure 7. λo (a) and So (b) calculated from standard overfilled CD measurement, compared to calculated values from offset launch measurements.

The utilization of $P(r)$ allows us to develop a method that uses the standardized launch conditions of 10 representative VCSEL that are already utilized for the worst case modal bandwidth computation [6]. Other launch conditions, such as encircled flux and overfill compliant conditions can be utilized to evaluate the range of variation of the CD parameters. Figure 8 summarizes the calculated λo and So as a function of the ten VCSEL weights used in modal bandwidth standards.

In Figure 9, results from two samples (B1, C1) are investigated in more detail. λo and So values are plotted for individual offsets, for the ten VCSEL weighted sums, OFLc weighted sums, and the actual OFL measurement results. Given the varying level of spatial profiles from VCSEL weights, they span a range of λo, So values, approaching that of OFLc weights. Although the weighted λo, So values do not coincide exactly on the offset values, they show identical So/λo slopes. The small bias between weighted results and the actual offset results are attributed to errors from weighting calculations, and they seem to be insignificant for this study. As noted earlier in section 3.2, Figure 9 shows about 4 ps/nm/km dispersion

difference at 850nm, between LOMs and HOMs, for all fibers tested. This shows the impact of the extreme launch conditions and generally does not happen in practice.

An important launch condition that is developed for better reproducible link and channel insertion loss requires Encircled Flux (EF) compliance. One can see from Figure 9 that the CD results from more optimistic OFL launch are not too far from more realistic EF launch case. Although it is desirable to change the CD measurement launch condition to EF compliant launch to align this measurement with other MMF measurements, not doing so does not create considerable error according to Figure 9.

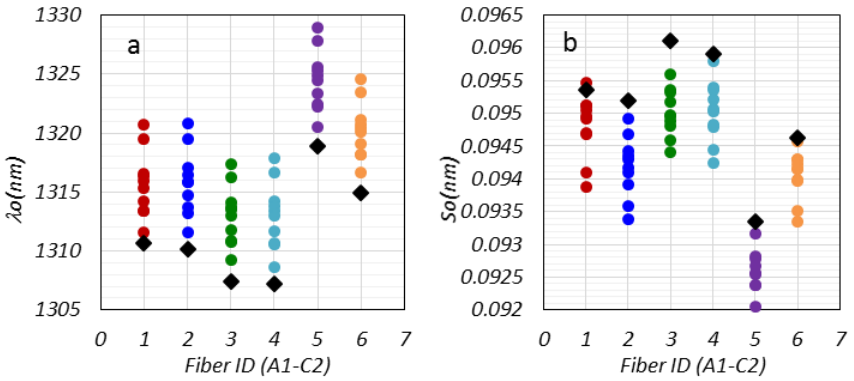

Figure 8. λ₀ (a) and So (b) calculated by scaling the radial offset launch measurements data. Black diamonds show the results of OFLc weights, corresponding to overfilled launch. Colored dots show ten VCSEL weights, with varying degree of underfilling. A suitable encircled flux compliant launch would result somewhere between worst VCSEL and OFLc weight.

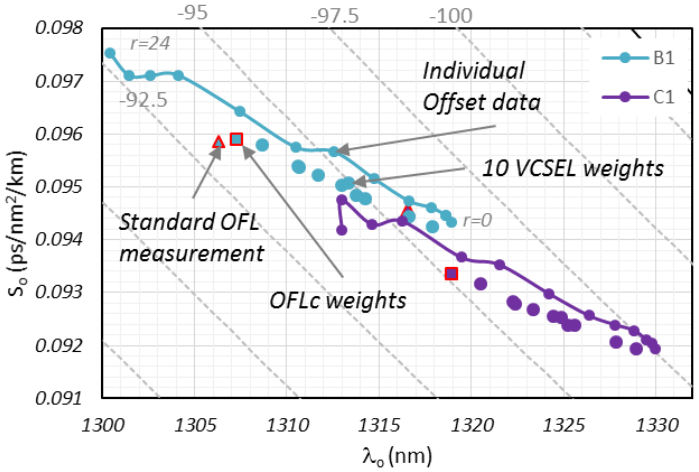

Figure 9. A closer look at two of the fiber samples (B1, C1) CD measurements. Results based on scaling with 10 VCSEL weights with underfilled and slightly overfilled launch track well with the individual radial offset values (with a certain bias, that can be calculation related).

Impact on Channel Performance

As application speeds increase, the spectral width of VCSEL transceivers gets broader, increasing the channel chromatic dispersion (CD) impairment (ex. 40/100GBASE-SR4/SR10: 0.65 nm 10GBASE-SR: 0.45 nm). In Figure 10 we show the maximum calculated channel reach as a function of spectral width using the IEEE link model where 100GBASE-SR4 channels are limited to 100m due to chromatic dispersion.

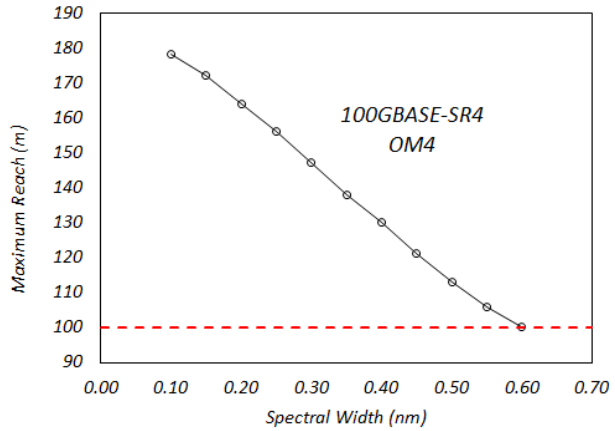

Figure 10. Channel reach as a function of VCSEL spectral width for 100GBASE-SR4.

Conclusions

Modeling and experiment results presented in this paper show that each mode group of the MMF has a distinct zero dispersion wavelength. This MMF property could produce errors in the characterization of the CD parameters (λ_o and S_o) as the results depend on launch condition. The errors for λ_o can be as high as 15nm. We show that by measuring CD at radial offsets and scaling the offset results with desirable launch condition scaling factors (e.g., OFLc, EF), MMF λ_o and So values more relevant to applications can be achieved.

The modeled and measured results can be applied not only for accurate characterization of CD, but also to the design of the MMF. In [4] it was shown that linear scaling of mode group delays is dependent on dopant concentrations. Modal CD characterization presented here can be used to tune the scaling factors, thereby simplifying the design or testing of the wideband MMF.

References

[1] G. Brown, “Chromatic dispersion measurement in graded-index multimode optical fibers,” J. Lightwave Tech., 12 (11), pp. 1907-1909, Nov. 1994.

[2] J. Carpenter, T. D. Wilkinson, “Characterization of multimode fiber by selective mode excitation”, J. Lightwave Tech., 30(10), pp. 1386-1392, May 2012.

[3] M. J. Hackert, “Development of chromatic dispersion measurement on multimode fiber using the relative time of flight measurement technique”, Photonics Tech. Lett, 4(2), pp 198-200, Feb. 1992.

[4] TIA TR-42.11/12 WBMMF Joint Task Group

[5] B. Kose, J. Castro, R. Pimpinella, Y. Huang, A. Novick, “Zero Dispersion Modes and its Effects on Characterization of MMF Chromatic Dispersion,” OFC 2015, paper M2C.5.

[6] TIA-455-220-A, "Differential mode delay measurement of multimode fiber in the time domain."

[7] IEC 60793-1-42 Ed 2, “Optical fibres – Part 1-42: Measurement methods and test procedures – Chromatic dispersion.”

[8] O.V. Butov, K.M. Golanta, A.L. Tomashuka, M.J.N. van Stralenb, A.H.E. Breuls, “Refractive index dispersion of doped silica for fiber optics,” Optics Communications, 213 (2002) pp. 301–308, Oct. 2002.

About Panduit

Panduit enables data centers to realize their full potential through an integrated stack of physical and intelligent infrastructure solutions that drive actionable performance gains and efficiencies to reduce operating costs and maximize capacity of power, cooling, space, and connectivity for the greatest ROI. Bridging physical equipment (cabinets, copper and fiber connectivity, and pathways), intelligent solutions (monitored rack PDUs, intelligent patching, and DCIM software), and professional services, Panduit offers the most comprehensive integrated data center portfolios available from one single source vendor. Complemented further by strong technology partnerships, Panduit integrated data center solutions are designed to answer increasing demand for IT services and technologies, while simplifying growing complexity in the data center design.

www.panduit.com · cs@panduit.com

FBAT03--WW-ENG, Rev 0, 06/2017